

Application of Absorbing Boundary Condition to Nuclear Breakup Reactions

M. Ueda* and K. Yabana†

Institute of Physics, University of Tsukuba, Tsukuba 305-8571, Japan

T. Nakatsukasa‡

Department of Physics, Tohoku University, Sendai 980-8578, Japan

(Dated: November 2, 2018)

Abstract

Absorbing boundary condition approach to nuclear breakup reactions is investigated. A key ingredient of the method is an absorbing potential outside the physical area, which simulates the outgoing boundary condition for scattered waves. After discretizing the radial variables, the problem results in a linear algebraic equation with a sparse coefficient matrix, to which efficient iterative methods can be applicable. No virtual state such as discretized continuum channel needs to be introduced in the method. Basic aspects of the method are discussed by considering a nuclear two-body scattering problem described with an optical potential. We then apply the method to the breakup reactions of deuterons described in a three-body direct reaction model. Results employing the absorbing boundary condition are found to accurately coincide with those of the existing method which utilizes discretized continuum channels.

PACS numbers: 24.10.-i, 24.50.+g, 25.70.Mn

*Electronic address: mueda@nucl.ph.tsukuba.ac.jp

†Electronic address: yabana@nucl.ph.tsukuba.ac.jp

‡Electronic address: takashi@nucl.phys.tohoku.ac.jp

I. INTRODUCTION

In nuclear reactions with weakly-bound projectiles, breakup processes are significant not only for their prominent cross sections as a final reaction product but also for their influences on other reaction channels such as elastic scattering. The breakup processes have been investigated originally for the reactions involving weakly-bound stable nuclei, such as deuterons [1, 2] and $^{6,7}\text{Li}$ [3]. In the last decade, interests on the breakup reactions have explosively increased because of the discovery of the halo nuclei around the neutron drip-line and the studies of their reactions [4].

A variety of theories have been developed to describe the breakup processes. In this article, we consider reactions in which the weakly-bound projectile is described as a composite two-body system and the whole reaction is described as a three-body problem of the projectile and the target. At sufficiently high incident energies, one may assume that the projectile internal motion is much slower than the projectile-target relative motion. Then, the projectile internal motion may be frozen during the reaction. This is the adiabatic approximation, which has been developed originally for the deuteron reactions [5]. One may also adopt the eikonal approximation for the fast projectile-target relative motion. A combined use of the eikonal and adiabatic approximations has provided especially useful descriptions for the reactions of halo nuclei [6].

For a more accurate description, a fully quantum mechanical treatment of the breakup processes has been developed in a coupled channel framework. This is known as the coupled discretized continuum channels (CDCC) method [1, 2, 3]. In this method, the continuum excited states of the projectile are incorporated by discretizing the momentum variables. The CDCC method has been successful in describing the reactions of deuterons [1, 2] and $^{6,7}\text{Li}$ [3], and has been recently applied to the reactions of halo nuclei [7].

In the present article, we discuss an alternative, fully quantum mechanical method: the method of absorbing boundary condition (ABC). This method was developed in the field of chemical reactions [8, 9, 10]. The key ingredient is an introduction of the absorbing potential outside the physically relevant area. This absorbing potential allows us to treat scattering problems with the vanishing boundary condition. We show that the ABC method provides a useful description for the breakup reactions in which the final scattering channels include three-body continuum states.

The present article is organized as follows: In Section II, we illustrate the ABC method in the simplest example, a two-body scattering problem with a nuclear optical potential. In Section III, we formulate the ABC method for three-body scattering problems. In Section IV, we present results of the ABC method applied to the breakup reaction of $d+^{58}\text{Ni}$ at the incident deuteron energy of 80 MeV. The results are then compared with those by the CDCC method. The summary is given in Section V.

II. ABSORBING BOUNDARY CONDITION METHOD: A POTENTIAL SCATTERING

We first explain the ABC method considering the simplest example: the scattering of a particle of mass m from a potential $V(\mathbf{r})$. We separate the potential $V(\mathbf{r})$ into two parts,

$$V(\mathbf{r}) = V_0(\mathbf{r}) + \Delta V(\mathbf{r}). \quad (1)$$

The potential $V_0(\mathbf{r})$ is spherical and may be of long-range. We assume that it is easy to construct the scattering solution $\psi_0^{(+)}(\mathbf{r})$ for the potential $V_0(\mathbf{r})$. The potential $\Delta V(\mathbf{r})$ may not be spherical but must be of short-range, $\Delta V(\mathbf{r}) = 0$ for the spatial region beyond a certain radius r_c , $|\mathbf{r}| > r_c$.

The scattering wave function can be written in a form

$$\psi^{(+)}(\mathbf{r}) = \psi_0^{(+)}(\mathbf{r}) + \Delta\psi^{(+)}(\mathbf{r}) . \quad (2)$$

The function $\Delta\psi^{(+)}(\mathbf{r})$ is expressed by

$$\Delta\psi^{(+)}(\mathbf{r}) = \int d\mathbf{r}' G_0^{(+)}(\mathbf{r}, \mathbf{r}') \Delta V(\mathbf{r}') \psi^{(+)}(\mathbf{r}') = \int d\mathbf{r}' G^{(+)}(\mathbf{r}, \mathbf{r}') \Delta V(\mathbf{r}') \psi_0^{(+)}(\mathbf{r}'), \quad (3)$$

where $G_0^{(+)}(\mathbf{r}, \mathbf{r}')$ and $G^{(+)}(\mathbf{r}, \mathbf{r}')$ are the Green's functions with the potentials $V_0(\mathbf{r})$ and $V(\mathbf{r})$, respectively,

$$G_0^{(+)} = \frac{1}{E + i\epsilon - T_{\mathbf{r}} - V_0}, \quad G^{(+)} = \frac{1}{E + i\epsilon - T_{\mathbf{r}} - V}. \quad (4)$$

Here, $T_{\mathbf{r}}$ is the kinetic energy operator. A positive infinitesimal number ϵ specifies the outgoing-wave boundary condition. For the special case of $V_0 = 0$ with $\Delta V = V$, $\psi_0^{(+)}(\mathbf{r})$ becomes a plane wave and we have an analytic expression for $G_0^{(+)}$.

Now, let us explain the ABC method to construct the wave function $\Delta\psi^{(+)}(\mathbf{r})$. The basic trick is that the positive infinitesimal number ϵ is replaced by a finite, space-dependent

function $\epsilon(\mathbf{r})$. In order to simulate the outgoing boundary condition, we introduce the function $\epsilon(\mathbf{r})$ which is positive and finite in the spatial region, $r_c \leq r \leq r_c + \Delta r$. We impose the vanishing boundary condition at $r = r_c + \Delta r$ for $\Delta\psi^{(+)}(\mathbf{r})$. If the absorbing potential works ideally, only the outgoing waves are allowed in the spatial region around $r = r_c$. If we regard $\epsilon(\mathbf{r})$ as a part of the Hamiltonian, namely $\mathcal{H} = T_{\mathbf{r}} + V - i\epsilon(\mathbf{r})$, one may regard this replacement as an addition of the absorbing potential, $-i\epsilon(\mathbf{r})$, to the Hamiltonian, $H = T_{\mathbf{r}} + V$.

Employing the absorbing potential $\epsilon(\mathbf{r})$, we can rewrite Eq. (3) for $\Delta\psi^{(+)}(\mathbf{r})$ as the following linear inhomogeneous equation,

$$(E + i\epsilon(\mathbf{r}) - T_{\mathbf{r}} - V)\Delta\psi^{(+)}(\mathbf{r}) = \Delta V(\mathbf{r})\psi_0^{(+)}(\mathbf{r}), \quad (5)$$

where, as mentioned above, the scattered wave $\Delta\psi^{(+)}(\mathbf{r})$ should satisfy the vanishing boundary condition at $r = r_c + \Delta r$. The right hand side of this equation is spatially localized since we assume that the potential $\Delta V(\mathbf{r})$ vanishes in the spatial region $r > r_c$.

The ABC approach thus allows us to obtain the scattered wave function in the spatial region of $r < r_c$ by imposing the vanishing boundary condition at $r = r_c + \Delta r$. We should note that no asymptotic form is required to solve the scattering problem in this procedure. The elastic scattering amplitude $f(\hat{\mathbf{k}})$ can be obtained from the wave function in the spatial region where the potential $\Delta V(\mathbf{r})$ exists,

$$f(\hat{\mathbf{k}}) = f_0(\hat{\mathbf{k}}) - \frac{m}{2\pi\hbar^2} \int d\mathbf{r} \psi_{0\mathbf{k}}^{(-)*}(\mathbf{r}) \Delta V(\mathbf{r}) \psi^{(+)}(\mathbf{r}), \quad (6)$$

where $f_0(\hat{\mathbf{k}})$ is the scattering amplitude with the potential $V_0(\mathbf{r})$ and $\psi_{0\mathbf{k}}^{(-)}(\mathbf{r})$ is the incoming-wave solution in the potential $V_0(\mathbf{r})$ with the incident momentum \mathbf{k} ($k = \sqrt{2mE}/\hbar$ and $\hat{\mathbf{k}} = \mathbf{k}/k$). Here, the wave functions are normalized as $|\psi(\mathbf{r})| \rightarrow 1$ at $r \rightarrow \infty$.

The accuracy of the calculated solution depends on the quality of the absorbing potential. One should choose the function $\epsilon(\mathbf{r})$ carefully to make the reflected waves as small as possible. In this respect, the absorbing potential with linear dependence on the coordinate has been tested extensively [11, 12]. We parameterize the potential as

$$-i\epsilon(\mathbf{r}) = \begin{cases} 0 & (r < r_c) \\ -iW_{\text{abs}} \frac{r-r_c}{\Delta r} & (r_c \leq r \leq r_c + \Delta r) \end{cases}, \quad (7)$$

where W_{abs} , r_c , and Δr are positive constants, representing the strength, radius, and thickness of the absorbing potential, respectively. The absorbing potential should be sufficiently strong to absorb all the outgoing waves, and should be smooth enough to avoid the occurrence of the significant reflected waves. These conditions could be fulfilled if we employ a large enough value for Δr . The large Δr , however, implies the necessity of treating a large spatial area, which in turn results in the increase of the computational task. In practice, the following condition derived in the WKB approximation, gives a criterion for a good absorber [11, 12]:

$$20 \frac{\hbar E^{1/2}}{\Delta r \sqrt{8m}} < W_{\text{abs}} < \frac{1}{10} \Delta r \frac{\sqrt{8m} E^{3/2}}{\hbar}. \quad (8)$$

The left inequality of Eq. (8) originates from the condition that the absorption is strong enough to suppress any reflection at $r = r_c + \Delta r$, while the right inequality originates from the condition that the reflection at $r = r_c$ is sufficiently small. Lower the bombarding energy E becomes, the wider Δr is required to fulfill the condition of Eq. (8). This is due to the increase of the de-Broglie wave length at low energies.

In order to demonstrate the quality of the ABC calculation, we consider, as an example, the elastic scattering of $^{16}\text{O} + ^{12}\text{C}$ at $E_{\text{lab.}} = 139.2$ MeV with the optical potential of Ref. [13]. The potential $V(\mathbf{r})$ is spherical and composed of the real and imaginary parts of the nuclear potential and of the Coulomb potential whose short range part is regularized with a quadratic function (the Coulomb potential of a uniformly charged sphere).

Although one can easily obtain the numerical solution for the potential $V(\mathbf{r})$, we divide the potential into two parts, $V_0(r)$ and $\Delta V(r)$, in order to test the ABC. Here, we adopt the real part of the nuclear potential as $\Delta V(r)$, and the rest as $V_0(r)$. We solve Eq. (5) in the partial wave expansion, $\Delta\psi^{(+)}(\mathbf{r}) = \sum_{lm} (y_l(r)/r) Y_{lm}(\hat{\mathbf{r}})$.

We fix the parameters of the absorbing potential, Eq. (7), as $r_c = 20$ fm and $\Delta r = 10$ fm, but vary W_{abs} . The vanishing boundary condition, $y_l(r) = 0$, is imposed at $r = r_c + \Delta r = 30$ fm. The discrete variable representation, which will be explained in detail in Section III, is utilized with the uniform grid spacing of 0.2 fm.

In Fig. 1 (a), we show absolute values of the S -matrices as a function of l calculated with different values of W_{abs} . The closed circles represent the absolute values of the S matrices which are obtained by a standard numerical procedure to integrate the radial Schrödinger equation up to $r = 30$ fm. One can see that the ABC method works quite well in describing

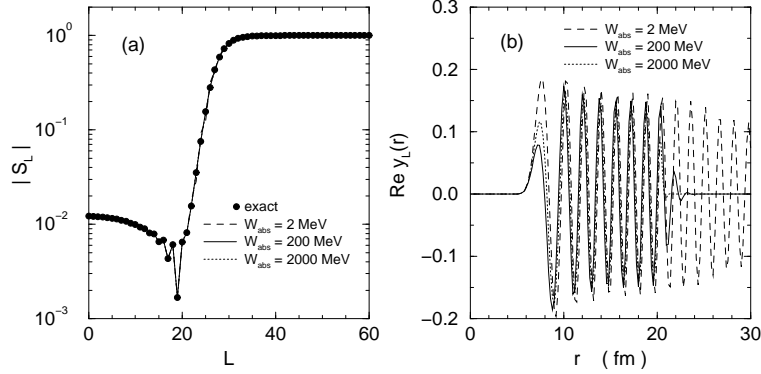


FIG. 1: (a) The absolute values of the S -matrices as a function of the relative angular momentum l for the elastic $^{16}\text{O} + ^{12}\text{C}$ scattering at $E_{\text{Lab.}} = 139.2$ MeV. (b) The real part of the radial wave function of the scattering partial wave $l = 30$.

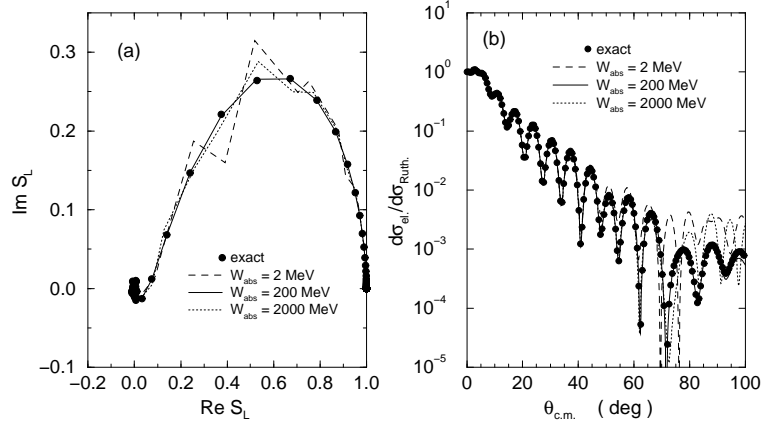


FIG. 2: The elastic scattering S matrix elements S_l (a) and the differential cross section (b) for the same reactions as shown in Fig. 1.

the potential scattering. It should be noted that only the absorbing potential with $W_{\text{abs}} = 200$ MeV satisfies the condition of Eq. (8).

In Fig. 1 (b), we show the real part of $y_l(r)$ for the partial wave of $l = 30$, which corresponds to the grazing angular momentum. The three lines correspond to the different choices of the strength W_{abs} . The damping behavior of the three wave functions in the region $20 \leq r \leq 30$ fm are different according to the strength W_{abs} . Despite of small deviation in the wave functions at $r < 20$ fm, it does not affect the absolute values of the elastic scattering S matrix elements as we saw above. This implies that the reaction cross section is not so sensitive to the choice of the absorbing potential.

However, when evaluating the differential cross sections, one has to be careful on the choice of the absorbing potential. Figure 2 displays the Argand diagram of the elastic scattering S matrix elements (*a*), and the differential cross sections (*b*). The elastic scattering cross sections in the Rutherford ratio vary by a few orders of magnitude as a function of the scattering angle. The subtle difference in the scattering matrix results in the substantial deviation in the differential cross sections. The calculation with $W_{\text{abs}}=200$ MeV, which fulfills the condition of Eq. (8), is reasonably accurate while the other choices of W_{abs} , which do not fulfill the condition, give less accurate results at large angles.

III. ABSORBING BOUNDARY CONDITION METHOD: A THREE-BODY REACTION

A. Basic equations

In this section we explain how to apply the ABC to three-body breakup reactions. We consider the reaction of a projectile (P) on a target (T), in which the projectile is composed of a core nucleus (C) and a neutron (n). We denote masses of the core, the neutron, and the target as m_C , m_n , and m_T , respectively. The charge numbers of the core and target are Z_C and Z_T , respectively. We employ a Jacobi coordinate system in which the n - C relative coordinate is denoted as \mathbf{r} and the P - T relative coordinate as \mathbf{R} . We assume that the total Hamiltonian is given by the following form,

$$H = -\frac{\hbar^2}{2\mu} \nabla_{\mathbf{R}}^2 - \frac{\hbar^2}{2m} \nabla_{\mathbf{r}}^2 + V_{nC}(\mathbf{r}_{nC}) + V_{nT}(\mathbf{r}_{nT}) + V_{CT}(\mathbf{r}_{CT}), \quad (9)$$

where the reduced masses, μ and m , of the relative P - T and n - C motions, respectively, are given by

$$\mu = \frac{(m_n + m_C)m_T}{(m_n + m_C) + m_T}, \quad m = \frac{m_n m_C}{m_n + m_C}. \quad (10)$$

The vectors

$$\mathbf{r}_{nC} = \mathbf{r}, \quad \mathbf{r}_{nT} = \mathbf{R} + \frac{m_C}{m_n + m_C} \mathbf{r}, \quad \mathbf{r}_{CT} = \mathbf{R} - \frac{m_n}{m_n + m_C} \mathbf{r}, \quad (11)$$

represent the n - C , n - T , and C - T separations, respectively. V_{nC} , V_{nT} , V_{CT} are the effective potentials between the corresponding particles. V_{CT} includes the Coulomb potential as well as the nuclear potential. V_{nT} and V_{CT} may be complex. Their imaginary parts represent excitations of the target and/or core nucleus. V_{nC} is assumed to be real.

We introduce an auxiliary distorting potential $U_{PT}(\mathbf{R})$ for the P - T relative motion. The $U_{PT}(\mathbf{R})$ may be chosen arbitrarily as long as it contains the long-range Coulomb part of the P - T interaction. The distorted wave function $\Phi_{\mathbf{K}}^{D(+)}(\mathbf{R})$ is a scattering solution of the following equation with the outgoing boundary condition,

$$\left[-\frac{\hbar^2}{2\mu} \nabla_{\mathbf{R}}^2 + U_{PT}(\mathbf{R}) \right] \Phi_{\mathbf{K}}^{D(+)}(\mathbf{R}) = E \Phi_{\mathbf{K}}^{D(+)}(\mathbf{R}), \quad \left(E = \frac{\hbar^2 \mathbf{K}^2}{2\mu} \right) \quad (12)$$

where \mathbf{K} is the incident wave number vector. In the partial wave expansion, we express $\Phi_{\mathbf{K}}^{D(+)}(\mathbf{R})$ as

$$\Phi_{\mathbf{K}}^{D(+)}(\mathbf{R}) = 4\pi \sum_{LM} i^L e^{i(\sigma_L + \delta_L)} \frac{f_L(K, R)}{KR} Y_{LM}^*(\hat{\mathbf{K}}) Y_{LM}(\hat{\mathbf{R}}). \quad (13)$$

For the n - C motion described with the Hamiltonian $h_{nC} = -\frac{\hbar^2}{2m} \nabla_{\mathbf{r}}^2 + V_{nC}(\mathbf{r})$, we denote the solutions as $\phi_{\beta}(\mathbf{r})$, where β specifies the quantum numbers $n_{\beta} l_{\beta} m_{\beta}$ for the bound orbitals and $k_{\beta} l_{\beta} m_{\beta}$ for the continuum states. n_{β} is the nodal quantum number and k_{β} is the magnitude of the wave number. l_{β} and m_{β} are the orbital angular momentum quantum numbers as usual. In the polar coordinate system, $\phi_{\beta}(\mathbf{r})$ is rewritten as

$$\phi_{\beta}(\mathbf{r}) = \frac{u_{\beta}(r)}{r} Y_{l_{\beta} m_{\beta}}(\hat{\mathbf{r}}), \quad (14)$$

where $u_{\beta} = u_{n_{\beta} l_{\beta}}$ for the bound orbitals and $u_{\beta} = u_{k_{\beta} l_{\beta}}$ for the continuum states. The bound wave function is normalized as usual, and the continuum wave function is normalized by the following asymptotic form,

$$u_{k_{\beta} l_{\beta}}(r) \sim \sqrt{\frac{2}{\pi}} \sin \left(k_{\beta} r - \frac{l_{\beta}}{2} \pi + \delta_{l_{\beta}} \right), \quad \text{at } r \rightarrow \infty, \quad (15)$$

where $\delta_{l_{\beta}}$ is the phase shift for the n - C scattering.

We express the total wave function $\Psi_{\mathbf{K}_0 \alpha}^{(+)}(\mathbf{R}, \mathbf{r})$ as the sum of the distorted wave in the incident channel α and a scattered wave as

$$\Psi_{\mathbf{K}_0 \alpha}^{(+)}(\mathbf{R}, \mathbf{r}) = \Phi_{\mathbf{K}_0}^{D(+)}(\mathbf{R}) \phi_{\alpha}(\mathbf{r}) + \Psi_S(\mathbf{R}, \mathbf{r}), \quad (16)$$

where \mathbf{K}_0 is the incident wave number vector of the P - T relative motion.

The scattered wave function $\Psi_S(\mathbf{R}, \mathbf{r})$, satisfies the following equation

$$(E - H) \Psi_S(\mathbf{R}, \mathbf{r}) = \Delta V(\mathbf{R}, \mathbf{r}) \Phi_{\mathbf{K}_0}^{D(+)}(\mathbf{R}) \phi_{\alpha}(\mathbf{r}), \quad (17)$$

with

$$\Delta V(\mathbf{R}, \mathbf{r}) = V_{nT}(\mathbf{r}_{nT}) + V_{CT}(\mathbf{r}_{CT}) - U_{PT}(\mathbf{R}), \quad (18)$$

where E is the total energy which is equal to the sum of the energies of the incident P - T relative motion $\hbar^2 \mathbf{K}_0^2 / 2\mu$ and the energy of the n - C relative motion in the incident channel, ϵ_α . The right hand side, $\Delta V(\mathbf{R}, \mathbf{r}) \Phi_{\mathbf{K}_0}^{D(+)}(\mathbf{R}) \phi_\alpha(\mathbf{r})$, should be localized in space. In other words, this function vanishes if either R or r is larger than a certain critical radius, R_C for R and r_c for r [23].

Since the scattered wave function, $\Psi_S(\mathbf{R}, \mathbf{r})$, includes only the outgoing waves asymptotically, it should be legitimate to simulate the outgoing boundary condition by introducing the absorbing potentials for both R and r coordinates. Thus, instead of solving Eq. (17) with the outgoing boundary condition, we propose to employ the following equation with the vanishing boundary condition.

$$[E + i\epsilon_{nC}(r) + i\epsilon_{PT}(R) - H] \Psi_S(\mathbf{R}, \mathbf{r}) = \Delta V(\mathbf{R}, \mathbf{r}) \Phi_{\mathbf{K}_0}^{D(+)}(\mathbf{R}) \phi_\alpha(\mathbf{r}), \quad (19)$$

where $\epsilon_{nC}(r)$ and $\epsilon_{PT}(R)$ are the absorbing potentials for the relative motions of n - C and P - T , respectively. They are placed in the spatial region $R > R_C$ for $\epsilon_{PT}(R)$, and $r > r_C$ for $\epsilon_{nC}(r)$. In practice, we employ the linear absorbing potentials of Eq. (7) for both functions. The vanishing boundary condition is imposed for $\Psi_S(\mathbf{R}, \mathbf{r})$ at $R = R_C + \Delta R$ and $r = r_C + \Delta r$. In this way, the three-body scattering problem is converted into the three-body Schrödinger-like equation with the vanishing boundary condition. No explicit consideration on the boundary conditions for three-body continuum states is required in this approach.

As for the parameters of the absorbing potentials, careful considerations are required. For $i\epsilon_{PT}(R)$, we choose the potential parameters according to the condition of Eq. (8), where the energy E may be evaluated at the relative P - T energy in the incident channel. However, for $i\epsilon_{nC}(r)$, the energy of n - C motion after reaction is not unique but spreads over a certain energy region. A reasonable choice is then to set the parameters of $i\epsilon_{nC}(r)$ optimum for the main component of the n - C motion. It should, however, be noted that the complete absorption of the breakup waves is difficult for small n - C relative energies because of their long wavelengths.

The three-body wave function obtained in the above procedure is meaningful in the inner spatial region, $r < r_C$ and $R < R_C$. The wave function only in this interacting region is required to calculate the relevant T -matrices. For the breakup processes in which the final n - C motion is specified by the relative wave number \mathbf{k} and the final P - T motion specified

by \mathbf{K} , the relevant T -matrices are given by

$$T_\alpha(\mathbf{K}, \mathbf{k}) = \langle \Phi_{\mathbf{K}}^{D(-)}(\mathbf{R}) \phi_{\mathbf{k}}^{(-)}(\mathbf{r}) | V_{nT} + V_{CT} - U_{PT} | \Psi_{\mathbf{K}_0\alpha}^{(+)}(\mathbf{R}, \mathbf{r}) \rangle, \quad (20)$$

where $\phi_{\mathbf{k}}^{(-)}(\mathbf{r})$ is the n - C wave function with the incident plane wave specified by the wave number vector \mathbf{k} and with the incoming boundary condition. This is related to $\phi_{klm}(\mathbf{r})$ of Eq. (14) by

$$\phi_{\mathbf{k}}^{(-)}(\mathbf{r}) = \sum_{lm} \frac{(2\pi)^{3/2}}{k} i^l e^{-i\delta_l} \phi_{klm}(\mathbf{r}) Y_{lm}^*(\hat{\mathbf{k}}), \quad (21)$$

where δ_l is the phase shift for the n - C scattering. For convenience, we introduce an alternative definition for the T -matrices, $T_{\alpha'\alpha}(\mathbf{K})$, in which α' specifies the final $n - C$ state, $\alpha' = nlm$ for the bound orbitals and $\alpha' = klm$ for the continuum states. This T -matrix is given by

$$T_{\alpha'\alpha}(\mathbf{K}) = \langle \Phi_{\mathbf{K}}^{D(-)}(\mathbf{R}) \phi_{\alpha'}(\mathbf{r}) | V_{nT} + V_{CT} - U_{PT} | \Psi_{\mathbf{K}_0\alpha}^{(+)}(\mathbf{R}, \mathbf{r}) \rangle. \quad (22)$$

For the reactions in which the final state is the three-body continuum state specified by $\alpha' = klm$, the T -matrices of Eqs. (20) and (22) are related by

$$T_\alpha(\mathbf{K}, \mathbf{k}) = \frac{(2\pi)^{3/2}}{k} \sum_{lm} (-i)^l e^{i\delta_l} Y_{lm}(\hat{\mathbf{k}}) T_{klm,\alpha}(\mathbf{K}). \quad (23)$$

Various cross sections can be expressed in terms of these T -matrices. For example, the angle-integrated elastic breakup cross section is given by

$$\sigma^{\text{breakup}} = \left(\frac{\mu}{2\pi\hbar^2} \right)^2 \sum_{lm} \int_0^\infty dk \frac{K}{K_0} |T_{klm,\alpha}(\mathbf{K})|^2. \quad (24)$$

B. Radial coupled channel equation

In practice, Eq. (19) is solved in the partial wave expansion. The incident wave function $\Phi_{\mathbf{K}_0}^{(+)}(\mathbf{R}) \phi_\alpha(\mathbf{r})$ and the total wave function $\Psi_{\mathbf{K}_0\alpha}^{(+)}(\mathbf{R}, \mathbf{r})$ are expressed as

$$\begin{aligned} \Phi_{\mathbf{K}_0}^{(+)}(\mathbf{R}) \phi_\alpha(\mathbf{r}) &= \sum_{JL} \sqrt{4\pi(2L+1)} \langle L0l_\alpha m_\alpha | Jm_\alpha \rangle i^L e^{i(\sigma_L + \delta_L)} \\ &\times \frac{f_L(K_0, R)}{K_0 R} \frac{u_{n_\alpha l_\alpha}(r)}{r} [Y_L(\hat{\mathbf{R}}) Y_{l_\alpha}(\hat{\mathbf{r}})]_{Jm_\alpha}, \end{aligned} \quad (25)$$

and

$$\begin{aligned} \Psi_{\mathbf{K}_0\alpha}^{(+)}(\mathbf{R}, \mathbf{r}) &= \sum_{JLL'\ell'} \sqrt{4\pi(2L+1)} \langle L0l_\alpha m_\alpha | Jm_\alpha \rangle i^L e^{i(\sigma_L + \delta_L)} \\ &\times \frac{y_{Ll_\alpha, L'\ell'}^J(R, r)}{R r} [Y_{L'}(\hat{\mathbf{R}}) Y_{\ell'}(\hat{\mathbf{r}})]_{Jm_\alpha}, \end{aligned} \quad (26)$$

respectively. For the scattered wave function $\Psi_S^{(+)}(\mathbf{R}, \mathbf{r})$, we make the same expansion as Eq. (26), replacing the radial wave function $y_{Ll_\alpha, L'l'}^J(R, r)$ with $\alpha_{Ll_\alpha, L'l'}^J(R, r)$. These two radial wave functions, $y_{Ll_\alpha, L'l'}^J(R, r)$ and $\alpha_{Ll_\alpha, L'l'}^J(R, r)$, are related to each other by

$$y_{Ll_\alpha, L'l'}^J(R, r) = \frac{1}{K_0} f_L(K_0, R) u_{n_\alpha l_\alpha}(r) \delta_{LL'} \delta_{l_\alpha l'} + \alpha_{Ll_\alpha, L'l'}^J(R, r). \quad (27)$$

The radial coupled-channel equation for the scattered wave function $\alpha_{Ll_\alpha, L'l'}^J(R, r)$ is written as

$$\begin{aligned} & \left[E + i\epsilon_{nC}(r) + i\epsilon_{PT}(R) \right. \\ & \left. - \left\{ -\frac{\hbar^2}{2\mu} \frac{\partial^2}{\partial R^2} + \frac{\hbar^2 L'(L'+1)}{2\mu R^2} - \frac{\hbar^2}{2m} \frac{\partial}{\partial r^2} + \frac{\hbar^2 l'(l'+1)}{2mr^2} + V_{nC}(r) \right\} \right] \alpha_{Ll_\alpha, L'l'}^J(R, r) \\ & - \sum_{L''l''} V_{L'l', L''l''}^J(R, r) \alpha_{Ll_\alpha, L''l''}^J(R, r) \\ & = \left\{ V_{L'l', Ll_\alpha}^J(R, r) - \delta_{LL'} \delta_{l_\alpha l'} U_{PT}(R) \right\} \frac{1}{K_0} f_L(K_0, R) u_{n_\alpha l_\alpha}(r), \end{aligned} \quad (28)$$

where the radial coupling potential $V_{L'l', L''l''}^J(R, r)$ is defined by

$$V_{L'l', L''l''}^J(R, r) = \int d\hat{\mathbf{R}} d\hat{\mathbf{r}} [Y_{L'}(\hat{\mathbf{R}}) Y_{l'}(\hat{\mathbf{r}})]_{JM}^* (V_{nT} + V_{CT}) [Y_{L''}(\hat{\mathbf{R}}) Y_{l''}(\hat{\mathbf{r}})]_{JM}. \quad (29)$$

The T -matrix elements are expressed in terms of the radial wave functions. For a transition concerning the n - C relative motion from the bound orbital $\alpha = n_\alpha l_\alpha m_\alpha$ in the incident channel to the continuum state $\alpha' = klm$ in the final channel, the relevant T -matrix element is expressed as

$$\begin{aligned} T_{\alpha'\alpha}(\mathbf{K}) &= \langle \Phi_{\mathbf{K}}^{D(-)}(\mathbf{R}) \phi_{\alpha'}(\mathbf{r}) | V_{nT} + V_{CT} - U_{PT} | \Psi_{\mathbf{K}_0\alpha}^{(+)}(\mathbf{R}, \mathbf{r}) \rangle \\ &= \sum_{JLL'} (4\pi)^{3/2} (2L+1)^{1/2} i^{L-L'} e^{i\sigma_L + i\sigma_{L'} + i\delta_L + i\delta_{L'}} \\ &\quad \times \langle L0l_\alpha m_\alpha | Jm_\alpha \rangle \langle L'm_\alpha - mlm | Jm_\alpha \rangle Y_{L'm_\alpha - m}(\hat{\mathbf{K}}) I_{\alpha'L', \alpha L}^J, \end{aligned} \quad (30)$$

where the radial integral $I_{\alpha'L', \alpha L}^J$ is given by

$$I_{\alpha'L', \alpha L}^J = \sum_{L''l''} \int_0^\infty dR dr \frac{1}{K} f_{L'}(K, R) u_{\alpha'}(r) \left\{ V_{L'l', L''l''}^J(R, r) - \delta_{L'L''} \delta_{l'l''} U_{PT}(R) \right\} y_{Ll_\alpha, L''l''}^J(R, r). \quad (31)$$

For the elastic channel in which the final state α' is identical to the initial one, $\alpha' = \alpha = n_\alpha l_\alpha m_\alpha$, the two-body T -matrix for U_{PT} should be added to the above expression of Eq. (30).

For later convenience, we present an expression for the angle-integrated elastic breakup cross section in terms of this radial integral. The elastic breakup cross section can be

decomposed into the sum over the total angular momentum J and the relative angular momentum l of the n - C motion, as well as the integral over the relative wave number k ,

$$\sigma^{\text{breakup}} = \sum_{Jl'l} \int_0^\infty dk \sigma_{Jl'l}^J(k), \quad (32)$$

with

$$\sigma_{Jl'l}^J(k) = 16\pi \left(\frac{\mu}{\hbar^2}\right)^2 \frac{K}{K_0} \left| \sum_L (2L+1)^{\frac{1}{2}} e^{i\delta_L + i\delta_{L'}} \langle L0l_\alpha m_\alpha | Jm_\alpha \rangle I_{\alpha'L',\alpha L}^J \right|^2, \quad (33)$$

where K is the P - T relative wave number which implicitly depends on the n - C wave number k through the energy conservation relation.

C. Computational details

To solve the radial coupled-channel equation (28), we discretize the radial variable with a uniform grid. To achieve high accuracy with a moderate number of grid points, we employ the so-called discrete variable representation (DVR) [14]. Although the DVR is a kind of basis expansion methods, the resultant equation is similar to that in the finite difference approximation.

We employ labels i and j for the grid points of the radial coordinates R and r , respectively. Denoting the grid spacings for the coordinates R and r as H and h , respectively, the grid points R_i and r_j are given by

$$R_i = i H, (i = 1 \dots N_R) \quad r_j = j h, (j = 1 \dots N_r), \quad (34)$$

where $R_c + \Delta R = N_R \cdot H$ and $r_c + \Delta r = N_r \cdot h$. The wave functions are then discretized as

$$[\alpha_{Ll_\alpha, L'l'}^J]_{ij} = \alpha_{Ll_\alpha, L'l'}^J(R_i, r_j). \quad (35)$$

In the DVR, the matrix elements of the potentials become diagonal,

$$[V_{Ll, L'l'}^J]_{ij, i'j'} = V_{Ll, L'l'}^J(R_i, r_j) \delta_{ii'} \delta_{jj'} . \quad (36)$$

The kinetic energy operator for the coordinate R is expressed as the following matrix form,

$$\left[-\frac{\hbar^2}{2\mu} \frac{d^2}{dR^2} \right]_{ij, i'j'} = \delta_{jj'} \frac{\hbar^2}{2\mu} D_{ii'}^R, \quad (37)$$

where $D_{ii'}^R$ is defined by

$$D_{ii'}^R = \frac{(-1)^{i-i'}}{H^2} \times \begin{cases} \frac{\pi^2}{3} - \frac{1}{2i^2} & \text{for } (i = i') \\ \frac{2}{(i-i')^2} - \frac{2}{(i+i')^2} & \text{for } (i \neq i') \end{cases} . \quad (38)$$

The kinetic energy operator for the radial coordinate r is expressed in a similar manner.

After these procedures, the radial coupled-channel equation, Eq. (28), is expressed as the following matrix form,

$$\sum_{L'l''i'j'} [A_{L'l',L'l''}^J]_{ij,i'j'} [\alpha_{Ll_\alpha,L'l''}^J]_{i'j'} = [b_{Ll_\alpha,L'l'}]_{ij} , \quad (39)$$

where the coefficient matrix $[A_{L'l',L'l''}^J]_{ij,i'j'}$ is defined by

$$\begin{aligned} [A_{L'l',L'l''}^J]_{ij,i'j'} = & E \delta_{L'L''} \delta_{l'l''} \delta_{ii'} \delta_{jj'} \\ & - \left\{ \frac{\hbar^2}{2\mu} D_{ii'}^R + \left(\frac{\hbar^2 L'(L'+1)}{2\mu R_i^2} - i\epsilon_{PT}(R_i) \right) \delta_{ii'} \right\} \delta_{jj'} \delta_{L'L''} \delta_{l'l''} \\ & - \left\{ \frac{\hbar^2}{2m} D_{jj'}^r + \left(\frac{\hbar^2 l'(l'+1)}{2mr_j^2} + V_{nC}(r_j) - i\epsilon_{nC}(r_j) \right) \delta_{jj'} \right\} \delta_{ii'} \delta_{L'L''} \delta_{l'l''} \\ & - V_{L'l',L'l''}^J(R_i, r_j) \delta_{ii'} \delta_{jj'} \end{aligned} \quad (40)$$

and the source term $[b_{Ll_\alpha,L'l'}]_{ij}$ is given by

$$[b_{Ll_\alpha,L'l'}]_{ij} = \left\{ V_{L'l',Ll_\alpha}^J(R_i, r_j) - \delta_{LL'} \delta_{ll_\alpha} U_{PT}(R_i) \right\} \frac{1}{K_0} f_L(K_0, R_i) u_{n_\alpha l_\alpha}(r_j) . \quad (41)$$

The dimension N_{dim} of this linear algebraic equation is given by the product of the number of angular momentum channels, which is denoted by N_J , the numbers of grid points N_R and N_r , i.e., $N_{\text{dim}} = N_J N_R N_r$. As will be seen in a practical example given in the next section, this dimension becomes as large as $N_{\text{dim}} = 10^5$. The coefficient matrix $[A_{L'l',L'l''}^J]_{ij,i'j'}$ is sparse, namely, the number of non-zero elements of this matrix is rather small.

There are many efficient algorithms which are proposed to solve such a linear algebraic equation with a sparse coefficient matrix. We will employ the Bi-conjugate gradient method [15], which is one of the most well-known iterative method to solve the linear algebraic equation with a complex non-hermitian coefficient matrix. In order to improve the convergence, the pre-conditioning [16] is carried out. In our problem, the diagonal part of the matrix \mathbf{A} includes huge elements because of the centrifugal barrier. In order to balance the matrix, we modify the equation as

$$\frac{1}{\sqrt{\mathbf{D}}} \mathbf{A} \frac{1}{\sqrt{\mathbf{D}}} \cdot \sqrt{\mathbf{D}} \vec{\alpha} = \frac{1}{\sqrt{\mathbf{D}}} \vec{b} , \quad (42)$$

where \mathbf{D} is the diagonal matrix whose elements are equal to the diagonal matrix elements of \mathbf{A} . The convergence of the Bi-conjugate gradient method is significantly accelerated for the matrix $\frac{1}{\sqrt{\mathbf{D}}}\mathbf{A}\frac{1}{\sqrt{\mathbf{D}}}$ compared with the original matrix \mathbf{A} .

After solving the equation, we calculate the T -matrices with the similar discretization.

IV. DEUTERON REACTIONS: COMPARISON WITH THE CDCC METHOD

We here apply the ABC method to the $d+^{58}\text{Ni}$ reaction at the incident deuteron energy $E_d = 80$ MeV. Since this reaction was studied in detail with the CDCC method [17], we can assess validity of the ABC method by comparing our results with those of Ref. [17].

We employ the same Hamiltonian as used in Ref. [17]. Namely, the global optical potential for nucleon-nucleus elastic scattering [18] is adopted as the interactions between the proton (neutron) in the deuteron and ^{58}Ni . The potentials at half of the incident deuteron energy is adopted. No spin-orbit force is taken into account. The potential parameters are: $V_R = 44.921$ MeV, $r_R = 1.17$ fm, $a_R = 0.75$ fm, $W_V = 6.100$ MeV, $W_{SF} = 2.214$ MeV, $r_I = 1.32$ fm, $a_I = 0.534$ fm for proton and $V_R = 42.627$ MeV, $r_R = 1.17$ fm, $a_R = 0.75$ fm, $W_V = 7.240$ MeV, $W_{SF} = 2.586$ MeV, $r_I = 1.26$ fm, $a_I = 0.534$ fm for neutron. The Coulomb potential of uniformly charged sphere is assumed between the centers of mass of the deuteron and ^{58}Ni . The radius of the sphere is set as 4.92 fm.

The potential for the p - n relative motion is taken as a Gaussian form, $V_{np}(r) = V_0 \exp[-r^2/a_0^2]$ with $V_0 = -72.15$ MeV and $a_0 = 1.484$ fm. The ground state is assumed to be a pure s -wave. This potential gives the deuteron binding energy of 2.22 MeV.

We treat the radial regions of R and r up to 50 fm. The radial scattered wave function $\alpha_{Ll_\alpha, L'l'}^J(R, r)$ is set equal to zero if either R or r is larger than 50 fm. The absorbing potentials $i\epsilon_{PT}(R)$ and $i\epsilon_{nC}(r)$ are active at $R, r > 25$ fm. They are parameterized as

$$i\epsilon_{PT}(R) = iW_{PT} \frac{R - R_c}{\Delta R}, \quad i\epsilon_{nC}(r) = iW_{nC} \frac{r - r_c}{\Delta r}, \quad (43)$$

with $W_{PT} = 50$ MeV, $R_c = 25$ fm, $\Delta R = 25$ fm, $W_{nC} = 20$ MeV, $r_c = 25$ fm, and $\Delta r = 25$ fm. This implies that the obtained solution will be reliable in the spatial region of $R, r < 25$ fm. As for the auxiliary distorting potential $U_{PT}(\mathbf{R})$, we take the folding potential in which the p - T and n - T potentials are folded with the deuteron ground state density.

We carry out the calculations for total angular momentum J up to 100, including $l = 0$

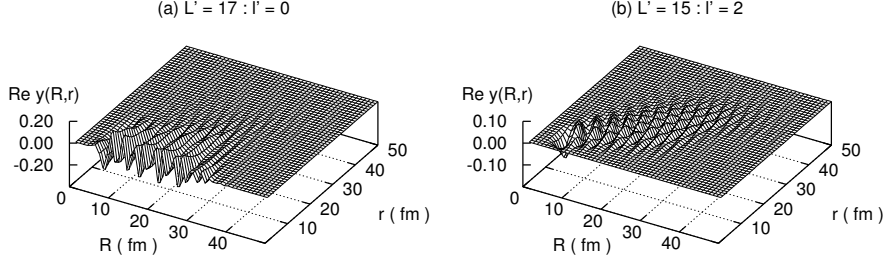


FIG. 3: (a) The real part of the radial wave function $y_{Ll_\alpha, L'l'}^J(R, r)$ for $J = 17$, $L' = 17$, and $l' = 0$ in the d - ^{58}Ni scattering at $E_d = 80$ MeV. (b) The same as (a) but for $J = 17$, $L' = 15$, and $l' = 2$.

and 2 for the p - n relative angular momentum. The radial discretization is made with a spacing of $H = 0.2$ fm for R and $h = 0.5$ fm for r . The matrix size is then given by the product of the number of angular momentum channel $N_J = 4$, the number of radial grid points $N_R = 250$ and $N_r = 100$. This amounts to the total number of points $N_{\text{dim}} = 10^5$. As mentioned in the previous section, we solve this linear algebraic problem with the sparse complex matrix using the Bi-conjugate-gradient method.

As for the grid spacing of the p - n coordinate, we found the spacing of 0.5 fm gives the accuracy of the deuteron binding energy better than 0.0001 MeV. The accurate binding energy by the n - p potential employed is 2.2177 MeV, while the DVR calculations with the grid spacing of 0.1 fm, 0.2 fm, and 0.5 fm give the same value of 2.2177 MeV.

In the present approach, we can explicitly obtain the wave function. In Fig. 3 (a), the real part of the radial wave function $y_{Ll_\alpha, L'l'}^J(R, r)$ is displayed for $J = L = L' = 17$, and $l' = l_\alpha = 0$. This includes the elastic scattering wave as well as the breakup waves. In the small r region the wave function is dominated by the elastic wave. It oscillates with the frequency close to K_0 in the coordinate of R . Its amplitude decreases as R increases in the region $R > 25$ fm, because of the absorption by $-i\epsilon_{PT}(R)$. The wave function at large r shows breakup components of the deuteron into the $p + n$ continuum state. The amplitude of the wave function also decreases at large r due to the absorption by $-i\epsilon_{nC}(r)$. Fig. 3 (b) shows the real part of $y_{Ll_\alpha, L'l'}^J(R, r)$ for $J = 17$, $L' = 15$, and $l' = 2$. For this angular momentum channel, only the breakup component is seen.

We next show decomposition of the breakup cross section $\sigma_{Ll}^J(k)$, which was defined in Eq. (33). Following Ref. [17], we show, in Fig. 4, the square moduli of the S -matrix, which

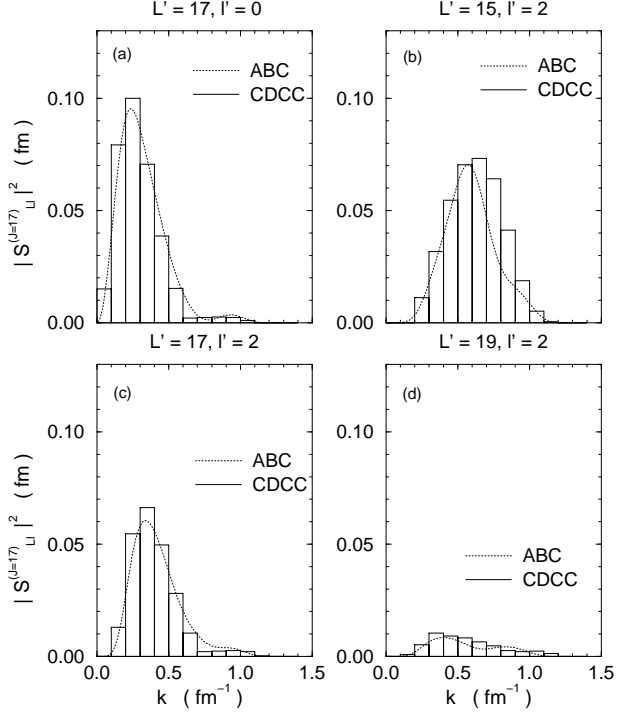


FIG. 4: (a) The squared moduli of the deuteron breakup S -matrix elements $|S_{L=Jl=0}^J|^2$. (b) $|S_{L=J-2l=2}^J|^2$. (c) $|S_{L=Jl=2}^J|^2$. (d) $|S_{L=J+2l=2}^J|^2$. In each panel, the dotted line and histogram denote the results of the ABC and CDCC methods, respectively.

are related to $\sigma_{Ll}^J(k)$ by $\sigma_{Ll}^J(k) = \frac{\pi(2J+1)}{K_0^2} |S_{Ll}^{(J)}(k)|^2$ for the present case ($l_\alpha = 0$). The deuteron s -wave breakup, $S_{L=Jl=0}^{(J)}(k)$, are shown in the panel (a) for $J = 17$. Three kinds of d -wave breakup S -matrix elements are shown in the panels (b) $S_{L=J-2l=2}^{(J)}(k)$, (c) $S_{L=Jl=2}^{(J)}(k)$, and (d) $S_{L=J+2l=2}^{(J)}(k)$, respectively. In each panel the dotted line and histogram represent the calculated results of the ABC and CDCC methods, respectively. The global behavior of the smooth dotted lines agrees well with that of the histogram [24]. We examined the sensitivity of the breakup cross sections against the strength of the absorbing boundary potential. We confirmed that the calculated results are not sensitive to these parameters, as long as the condition of Eq. (8) is satisfied.

We show in Table I the total reaction cross section σ_R and the elastic breakup cross sections σ_{BU} . The elastic breakup cross sections are decomposed according to the p - n relative angular momentum l . While the total reaction cross section σ_R and the s -wave breakup cross section $\sigma_{BU}^{(l=0)}$ calculated with the ABC method agree to those with the CDCC method, the d -wave breakup cross section $\sigma_{BU}^{(l=2)}$ of the ABC method is about 10 % smaller

TABLE I: Reaction and breakup cross sections of $d-^{58}\text{Ni}$ reaction at $E_d = 80$ MeV. The results of CDCC are taken from Ref. [17].

	$\sigma_{BU}^{(l=0)}$	$\sigma_{BU}^{(l=2)}$	σ_{BU}	σ_R
ABC	38.28 mb	77.21 mb	115.49 mb	1572.9 mb
CDCC	37.77 mb	88.59 mb	126.36 mb	1571.4 mb

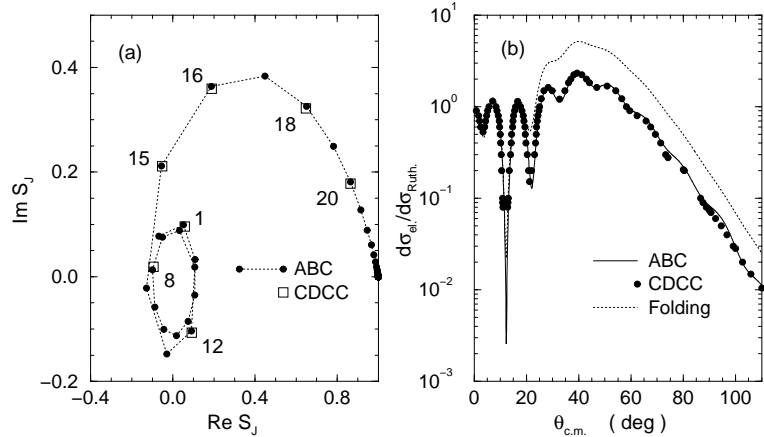


FIG. 5: The S -matrix (a) and differential cross section (b) of $d-^{58}\text{Ni}$ elastic scattering at $E_d = 80$ MeV. Results of the ABC are compared with those of the CDCC [1]. Results using a folding potential are also shown in (b).

than that of the CDCC method. This difference in $\sigma_{BU}^{(l=2)}$ is attributed to the difference seen in Fig. 4(b).

We next consider the angular distribution of the elastic scattering. Fig. 5 (a) shows the elastic scattering S -matrix elements S_J . The closed circles with dotted line denotes S_J calculated with the ABC methods. The open squares represent the corresponding CDCC results for $J = 1, 8, 12, 15, 16, 18$, and 20. Fig. 5 (b) shows the elastic scattering differential cross section in Rutherford ratio. The differential cross section calculated with the folding potential is also shown. The difference between the ABC (CDCC) calculations and the folding potential calculation shows the effect of the breakup process on the elastic scattering. The results clearly show that the ABC method gives almost the same results as the CDCC results. Therefore, the ABC method can describe the influence of the breakup processes on

the elastic scattering angular distribution.

V. SUMMARY

The purpose of the present article is to show the usefulness of the ABC method to describe nuclear breakup reactions. The basic trick in the method is to place an absorbing potential in the outer spatial region where complex three-body reactions do not take place. The vanishing boundary condition is imposed outside the absorbing potential. If the absorbing potential works properly, there exist only the outgoing waves at the edge of the interacting region where the absorbing potential is absent. We can thus obtain scattering solution by solving the Schrödinger-like equation with a source term, without imposing the scattering boundary condition.

In practical calculations, the equation is solved in the partial wave expansion, and the radial equation is discretized employing a uniform grid. The problem is then converted into the linear algebraic equation of large dimension with a complex, sparse, coefficient matrix. We can efficiently solve the equation by employing the Bi-conjugate-gradient method with a pre-conditioning procedure.

To show the feasibility and the accuracy of the ABC method, we have applied the method to the d - ^{58}Ni scattering as an example. For this scattering, detailed analyses with the CDCC method are available. We have found an excellent agreement between the results by the two methods, the ABC and the CDCC methods, for both breakup and elastic scattering. From this observation, we are confident that the physical contents of these two methods are the same, although the procedures in solving the three-body scattering problem look very different.

Let us compare the advantages and the limitations between the two methods. One of the superior features of the ABC method is that it is easy to assess convergence of the calculated results. If we fix the radial grid points and the number of partial waves for the n - C motion, the quality of the absorbing potential determines accuracy of the results. One can easily ascertain the reliability by examining how sensitive the results are to changes of the absorbing potential. The convergence check is more difficult in the CDCC method in which one must first prepare the discretized continuum wave functions. One must examine the delicate convergence as to the discretization of the continuum; the number of the momentum bins

and the maximum momentum to be incorporated.

The principal drawback of the ABC method is its heavy computational cost. One must solve a linear algebraic equation of large dimension. In the present example of deuteron reaction, one must solve the equation of 10^5 dimension for each angular momentum. For this problem, the computational time for each angular momentum is typically 20 minutes in a single alpha-21264 processor. This time multiplied by the number of angular momentum states gives the total computational time for the reaction at a fixed incident energy. Of course, the parallel computation would reduce the computational wall-time, by paralleling different angular momentum calculations.

In general, as the incident energy gets higher, the calculation becomes more demanding. This is because the finer grid spacing is required as the incident energy becomes higher. Also the number of angular momentum states that take part in the reaction increases. For reactions with heavy target nuclei, the Coulomb breakup reactions are significant, in particular when the projectile is bound extremely weak, such as the halo nuclei. The description of such Coulomb breakup reactions will be a difficult problem for the ABC method, because the coupling potential is so long-ranged that one should employ a large critical radius r_c to obtain reliable results. We must place the absorbing potential at a large radial distance, and must employ a large number of grid points. These difficulties are, however, not inherent in the ABC method, but are suffered by the other methods as well.

Establishing the usefulness of the ABC approach for breakup reactions of a weakly bound projectile, we are now planning to apply the method to reactions of unstable nuclei. A preliminary result on the nuclear breakup reactions of a single neutron halo nucleus, ^{11}Be , will be published in Ref. [20]. In that calculation, the number of the matrix size is about 2.4×10^5 , not so much different from that in the deuteron reaction. The ABC method should, at least, be useful for breakup reactions of a single nucleon halo nucleus induced by the nuclear force. Applicability of the ABC method depends on the availability of the computational facilities. We expect that the ABC method will be more popular and useful as the parallel computation becomes more prevalent.

The ABC method is also useful in any circumstances where the scattering boundary condition comes in. Some applications have been done and are in progress concerning resonances of a few-body system and response in the continuum, especially, of deformed systems [12, 21, 22].

Acknowledgments

One of the authors (T.N.) acknowledges the Grand-in-Aid for Scientific Research (No. 14740146) from the Japan Society for the Promotion of Science.

- [1] M. Yahiro, Y. Iseri, H. Kameyama, M. Kamimura and M. Kawai, *Prog. Theor. Phys. Suppl.* **89**, 32 (1986).
- [2] N. Austern, Y. Iseri, M. Kamimura, M. Kawai, G. Rawitscher and M. Yahiro, *Phys. Rep.* **154**, 125 (1987).
- [3] Y. Sakuragi, M. Yahiro and M. Kamimura, *Prog. Theor. Phys. Suppl.* **89**, 136 (1986).
- [4] I. Tanihata, *Prog. Part. Nucl. Phys.* 35 (1995) 505; *J. Phys.* **G22**, 157 (1996).
- [5] R.C. Johnson and P.J.R. Soper, *Phys. Rev.* **C1**, 976 (1970).
- [6] K. Yabana, Y. Ogawa, and Y. Suzuki, *Nucl. Phys.* **A539**, 295 (1992).
- [7] J. A. Tostevin, F. M. Nunes, and I. J. Thompson, *Phys. Rev.* **C63** (2001) 024617.
- [8] R. Kosloff and D. Kosloff, *J. Comp. Phys.* **63**, 363 (1986).
- [9] D. Neuhasuer and M. Baer, *J. Chem. Phys.* **90**, 4351 (1989).
- [10] T. Seideman and W.H. Miller, *J. Chem. Phys.* **97**, 2499 (1992).
- [11] M. S. Child, *Mol. Phys.* **72** (1991) 89.
- [12] T. Nakatsukasa and K. Yabana, *J. of Chem. Phys.* **114**, 2550 (2001).
- [13] M. E. Brandan, *Phys. Rev. Lett.* **60**, 784 (1988).
- [14] D.T. Colbert and W.H. Miller, *J. Chem. Phys.* **96**, 1982 (1992).
- [15] *e.g.* S. Fujino and S. -L. Zhang, “*Mathematical Science of Iterative Method*”, (Tokyo, Asakura, 1996) p. 51 (in Japanese)
- [16] *e.g.* Y. Fukui, T. Nodera, K. Kubota, and H. Togawa, “*Numerical Calculation*”, (Tokyo, Kyoritsu, 1999) p. 42 (in Japanese)
- [17] M. Yahiro, M. Nakano, Y. Iseri and M. Kamimura, *Prog. Theor. Phys.* **67**, 1467 (1982).
- [18] F. D. Becchetti and G. W. Greenlees, *Phys. Rev.* **182**, 1190 (1969).
- [19] T. Matsumoto, M. Yahiro and M. Kamimura, private communication.
- [20] K. Yabana, M. Ueda and T. Nakatsukasa, *Prog. Theor. Phys. Suppl.* in press.
- [21] T. Nakatsukasa and K. Yabana, Proceedings of the 7th International Spring Seminar on

Nuclear Physics, “*Challenges of Nuclear Structure*”, Maiori, Italy, May 2001
(World Scientific 2002), p.91.

- [22] T. Nakatsukasa and K. Yabana, Prog. Theor. Phys. Suppl. in press
- [23] The Coulomb potential could induce a long-range tail of $\Delta V(R, r)$ because of the difference between the center of mass and the center of charge for a projectile. An extended spatial region is required if the breakup reactions induced by this Coulomb field are significant.
- [24] There are small differences between the results obtained by the two methods, in particular, $S_{L=15l=2}^{J=17}$ around $0.7 \text{ fm}^{-1} < k < 1.0 \text{ fm}^{-1}$. The agreement of the results between the two methods becomes much better if the number of momentum bins is increased in the CDCC calculation [19].